Silicon impacts collagen remodelling and mineralization by human dental pulp stem cells in 3D pulp-like matrices

Daline Mbitta Akoa, Christophe Hélary, Asmaa Foda, Catherine Chaussain, Anne Poliard, Thibaud Coradin

Dental Materials 40 (2024) 1390–1399

Contents lists available at ScienceDirect

Dental Materials

journal homepage: www.elsevier.com/locate/dental

Silicon impacts collagen remodelling and mineralization by human dental pulp stem cells in 3D pulp-like matrices

Daline Mbitta Akoa [a], Christophe Hélary [a], Asmaa Foda [b], Catherine Chaussain [b,c], Anne Poliard [b], Thibaud Coradin [a,*]

[a] Sorbonne Université, CNRS, Laboratoire de Chimie de la Matière Condensée de Paris, Paris, France
[b] Université de Paris Cité, UR2496 Pathologies, Imagerie et Biothérapies Orofaciales, FHU-DDS-net, Dental School, Montrouge, France
[c] AP-HP Service de médecine bucco-dentaire, Hôpital Bretonneau, Paris, France

ARTICLE INFO

Keywords:
Calcium silicates
Silicic acid
Dental pulp stem cells
Reparative dentine

ABSTRACT

Objectives: Silicon-releasing biomaterials are widely used in the field of dentistry. However, unlike bone, very little is known about the role of silicon on dental tissue formation and repair. This study investigates the influence of silicic acid on the survival, differentiation and mineralizing ability of human dental pulp stem cells (hDPSCs) in 3D pulp-like environments

Methods: Dense type I collagen hydrogels seeded with hDPSCs were cultured over 4 weeks in the presence of silicic acid at physiological (10 μM) and supraphysiological (100 μM) concentrations. Cell viability and proliferation were studied by Alamar Blue and live/dead staining. The collagen network was investigated using second harmonic generation imaging. Mineral deposition was monitored by histology and scanning electron microscopy. Gene expression of mineralization- and matrix remodeling-associated proteins was studied by qPCR.

Results: Presence of silicic acid did not show any significant influence on cell survival, metabolic activity and gene expression of key mineralization-related proteins (ALP, OCN, BSP). However, it induced enhanced cell clustering and delayed expression of matrix remodeling-associated proteins (MMP13, Col I). OPN expression and mineral deposition were inhibited at 100 μM. It could be inferred that silicic acid has no direct cellular effect but rather interacts with the collagen network, leading to a modification of the cell-matrix interface.

Significance: Our results offer advanced insights on the possible role of silicic acid, as released by pulp capping calcium silicates biomaterials, in reparative dentine formation. More globally, these results interrogate the possible role of Si in pulp pathophysiology.

1. Introduction

First studies on pulp reactions to silicate-based filling materials date back to the 1940s, suggesting marked degenerative changes in pulp tissue [1,2]. Over the last decades, different calcium silicate (CS) materials exhibiting low toxicity, high biocompatibility and the ability to trigger the formation of mineralized tissue have been developed and launched on the market [3,4]. Their use as pulp-capping materials has become very common in dental clinical practice, as they are able to support dentin repair by promoting differentiation of dental pulp stem cells (DPSCs) into odontoblasts-like cells, as well as mineralization [5]. However, only a limited number of studies have attempted to define the molecular mechanisms mediating the response of DPSCs to these CS materials to form reparative dentin [6].

Emerging evidence supports that Ca^{2+} ions released by CS biomaterials are mobilized by DPSCs, leading to intracellular transcriptional changes in DPSCs during odontogenic differentiation, with increased mineralization [7,8]. However, studies demonstrated that the viability, proliferation and differentiation of DPSCs were enhanced in CS materials when compared with calcium hydroxide [9,10]. In a clinical study, the success rate of calcium hydroxide was 59 % at 2–3 years follow-up; in contrast, calcium silicates showed a success rate of 81–86 % [11]. This suggests that the superior effect of calcium silicates over calcium hydroxide might be attributed to the soluble silicon ($Si(OH)_4$, silicic acid) released by CS. When studying the effects of soluble silicon on DPSCs *in vitro*, supernatants obtained from the immersion of CS in the physiological medium were used as a source of silicon (Si) [10,12–14]. These solutions stimulated DPSCs proliferation and differentiation more

* Correspondence to: Sorbonne Université-CNRS, Paris, France.
E-mail address: thibaud.coradin@sorbonne-universite.fr (T. Coradin).

https://doi.org/10.1016/j.dental.2024.06.021
Received 15 March 2024; Received in revised form 14 June 2024; Accepted 14 June 2024
Available online 21 June 2024

than CH supernatant, suggesting that soluble Si released from CS positively influenced cells. However, CS extracts contain both $Si(OH)_4$ and Ca^{2+} ions, and thus the specific role of soluble Si on DPSC is still not established.

Unlike its role in dentin formation, Si influence on bone formation is well documented, although yet not fully understood [15–17]. It has been advocated that Si promotes bone formation and gene expression involved in cell osteoblastic differentiation, mineralization and type I collagen synthesis [18–21]. The concentration-response is still debated and may vary according to the cell type [22]. For example, increased calcium deposition and type 1 collagen gene expression by human osteosarcoma MG-63 was observed at a supra-physiological concentration of 4 mM Si [19]. Using the same cell line, the largest production of collagen was obtained with the addition of the physiological concentration of 10–20 μM Si in the culture medium, but the researchers did not find any change in type I collagen RNA level [18]. Similar study with osteoblasts revealed upregulated type I collagen gene expression with 50 μM Si [20]. Using mesenchymal stem cells, Si at a concentration of 625 μM significantly enhanced the proliferation, mineralization nodule formation, bone/tooth-related gene expression (osteocalcin, osteopontin and alkaline phosphatase) and synthesis of mineralization-related proteins (alkaline phosphatase and osteopontin) [23]. Such heterogeneity in the cellular response suggests that additional parameters beyond silicic acid concentration play a key role in Si ability to promote mineralization.

Conventionally, the cellular response to soluble silicon has been investigated *in vitro* in 2D cell culture. Although 2D culture research models offer a simple and cost-effective approach to maintaining cell culture, failure to mimic native tissue environment, changes in cell morphology and division, and disruption of interactions between the cells and the extracellular matrix raise the question of their physiological relevance [24]. 3D *in vitro* models have opened up new possibilities for modelling tissue interactions *in vivo*, enabling scientists to explore the biochemical cues underlying tissue formation. Cell-seeded dense, plastically-compressed collagen scaffolds have been validated as 3D cell culture models relevant to dental and bone biology, as they mimic the precursor matrices of tooth and bone mineralization, predentin and osteoid respectively [25–27]. Furthermore, they have the potential to guide DPSC odonto/osteoblastic differentiation and DPSC-mediated matrix mineralization both *in vitro* and *in vivo* [28–30].

In this context, the aim of this study was to investigate the effects of soluble silicon on reparative dentin formation using an *in vitro* model built from human DPSCs seeded in biomimetic 3D dense collagen hydrogels. Based on previous results obtained in a bone repair context [22], we hypothesized that the viability, odonto/osteogenic differentiation as well as mineralization and matrix remodelling activity of hDPSCs could be impacted by the presence of silicon. Moreover, we anticipated that the cellular response would vary with silicic acid concentration, especially depending on whether it was at physiological (10 μM) or supraphysiological (100 μM) level [31].

2. Materials and methods

2.1. Cell source

Human DPSCs were isolated from healthy teeth extracted from patients aged 15–20 years for orthodontic reasons at the AH-HP Bretonneau Hospital Dental Department. Teeth were collected according to the ethical guidelines established by French bioethics law (IRB agreement 00006477 and n° DC-2009–927, Cellule Bioéthique DGRI/A5), under an opt-out consent model. Primary DPSC were obtained following the extraction protocol established by Gronthos et al. [32]. Cells at passage 4 were used in this study.

2.2. Preparation of dense collagen hydrogels

Type I collagen was extracted from young rat tail tendons [33] to prepare dense 3D collagen gels using plastic compression, as previously described [28,34]. Briefly, type I collagen (4 $mg.mL^{-1}$) solubilised in a 20 mM acetic acid solution was mixed with DMEM 5X (Dulbecco's Modified Eagle Medium) and adjusted to the physiological pH with 0.1 M NaOH. After neutralization, hDPSCs suspended in a complete medium (DMEM media supplemented with 10 % fetal bovine serum and 1 % penicillin/streptomycin) were added to the collagen solution to obtain a pre-compression concentration of 2×10^6 $cells.mL^{-1}$ [30]. The mixture with a final collagen concentration of 1.6 $mg.mL^{-1}$ was then placed into a 24-well plate and incubated at 37 °C/5 % CO_2 for 30 min. The resulting highly hydrated collagen gels were transferred to a stack of blotting paper, nylon and stainless-steel mesh and loaded with a compressive stress of 1 kPa for 5 min, yielding dense collagen gel scaffolds (> 10 % w/v fibrillar collagen density) [34].

2.3. Cell culture conditions

The hDPSCs encapsulated in plastically compressed dense collagen hydrogels were grown in a mineralizing induction medium (MIM) made of 300 μM L-ascorbic acid sodium salt, 10 nM dexamethasone, 10 mM β-glycerophosphate, 10 % fetal bovine serum, and 1 % penicillin/streptomycin, without or with Si $(OH)_4$ at concentrations of 10 μM (Si10) or 100 μM (Si100). Stock solutions of concentrated silicic acid (x100) were previously prepared from a commercial standard solution (Silicon Standard for ICP, 1002 ± 2 $mg.L^{-1}$ in NaOH, Sigma Aldrich) and adjusted to physiological pH with HCl before being diluted in the mineralizing medium. Cell-laden collagen gels were cultured in 6-well plates using 5 mL of culture medium per well. Acellular gels cultured in MIM alone or supplemented with Si (10−100) were established as controls. Gels were incubated for 24 days, with differentiation media being renewed at 2- or 3-day intervals.

2.4. Cell viability, distribution and metabolic activity

Cell viability and distribution within the dense collagen gels were analysed by means of a Leica SP5 upright confocal (Leica DMI6000 Upright TCS SP5) coupled with a multiphoton laser scanning microscopy (Mai Tai multiphoton laser), which enabled the simultaneous acquisition of fluorescence and second-harmonic generation (SHG) signal [35]. Prior to imaging, seeded cells were stained on day 24 post-culture following the live/dead® viability-cytotoxicity assay instructions (Thermofisher, Waltham, MA, USA). Constructs were washed in phosphate buffered saline (PBS) and stained with 2 μM calcein-AM and 4 μM ethidium homodimer-1 solution. Live cells were stained in green and dead cells in red. A hybrid collector with a wavelength of 438 ± 24 nm (initial excitation of 880 nm) was used to detect the SHG signal of the corresponding collagen fibers and a 25x/0.95 water objective with a working distance of 2.5 mm was used to acquire the z-stacks for each sample. Image series were acquired with the Leica Application Suite X software. Live/dead cells volumes and collagen signals were analysed using ImageJ.

Cell metabolic activity in dense collagen gels was analysed by alamarBlue® assay (Sigma-Aldrich, St. Louis, MO, USA) up to day 21 of culture. The cell-laden gels were incubated in a complete culture media containing 10 $\mu g.mL^{-1}$ resazurin at 37 °C/5 % CO_2 for 3 h. Absorbances were read at wavelength of 570/600 nm with a UV/Vis Uvikon spectrophotometer. The reduction percentage of AlamarBlue was calculated according to the manufacturer's instructions.

2.5. Cell-mediated gel contractility assay

Collagen gel contraction was quantified by measuring gel diameter on days 1, 3, 7, 10 and 14 of culture. The gel size was compared with the

initial gel diameter. 4 gels were measured per condition.

2.6. Scanning electron microscopy (SEM) / Energy-dispersive x-ray spectroscopy (EDS)

First, gels were fixed with 4 % paraformaldehyde (PFA) and washed with 0.1 M sodium cacodylate/0.6 M sucrose buffer, before being dehydrated in a series of alcohol solutions and dried with supercritical CO_2. Dried samples were mounted on metallic holders and sputter-coated with gold (15 nm layer) for SEM analysis and carbon (20 nm layer) for EDS. Samples were analysed under a Hitachi S-3400 N microscope at accelerating voltage of 10 kV for SEM and 70 kV for EDS. Several pictures at different magnifications (1500–10,000x) were taken to examine microstructural features and chemical content.

2.7. Histological and Immunohistochemistry staining

After 24 days in culture, gels were fixed in a 4 % PFA solution, dehydrated, embedded in paraffin and cut into 7 μm thick sections. Prior to staining, sections were deparaffinized with toluene and rehydrated in ethanol solutions of decreasing concentrations, finishing with water. Cell distribution within the collagen matrix was assessed using Masson's trichrome staining. Calcium and phosphate deposits were detected by alizarin red and Von Kossa, respectively. Micrographs were acquired under a light microscope (DMLB, Leica).

For immunochemistry, sections were rehydrated and permeabilized with 0.05 % Tween 20 (diluted in ethylenediaminetetraacetic acid buffer) at 95 °C for 20 min and blocked with 5 % bovine serum albumin (BSA, ThermoFisher Scientific) in PBS (PBS 1X - BSA 5 %) for 1 h at room temperature. Sections were incubated overnight at 4° C with the following primary antibodies: Nestin (1:200 dilution, 19483–1-AP, Proteintech, USA) and Osteopontin (1:50 dilution, sc-21742, Santa Cruz, USA). The following day, sections were incubated for 1 h with Rhodamine Red™ - X goat anti-mouse IgG secondary antibody (1:200, R6393, Invitrogen, Canada) for OPN and Rhodamine Red™-X goat anti-rabbit IgG secondary antibody (1:200, R6394, Invitrogen, Canada) for Nestin. Nuclei were then counterstained with DAPI (1:1000, Thermo Fisher Scientific) and the multi-exposure images were acquired using bandpass filters appropriate for the red dye and blue DAPI.

2.8. qRT-PCR analyses

On days 0, 7, 14, and 21, cell-laden dense collagen gels were digested by collagenase, homogenized using Trizol® (Invitrogen, USA) and stored at − 80 °C prior to utilization. Total RNA content was extracted using the RNeasy Plus Mini Kit (Qiagen, Hilden, Germany) according to the manufacturer's instructions. For quantitative PCR, single-stranded RNA was transformed into complementary double-stranded DNA (cDNA) by reverse transcription. 1 μL of random primers (200uM) (Invitrogen) and 1 μL deoxyribonucleosides triphosphates(10 mM) (Invitrogen) were added to 10 μL RNA aliquots (around 300–500 ng). Following denaturation of secondary structure at 65 °C and primers binding, 5X reaction buffer, dithiothreitol (0.2 M) and Moloney murine leukemia virus (M-MLV) (Invitrogen) were added. After 60 min at 37 °C, the reaction was stopped by heating at 70 °C for 10 min. The resulting cDNAs were stored at − 20 °C until further use.

Real-time fluorescence analysis using SYBR Green Master Mix (Roche Diagnostics GmbH, Germany) was used to quantify the expression level of specific genes relative to GAPDH or 18 S rRNA housekeeping genes. The primers used in RT-qPCR are listed in the table below (Table 1). The reaction involved a succession of 40 cycles, each cycle including denaturation (95 °C, 30 s), annealing (60 °C, 30 s) and elongation with Taq polymerase (72 °C, 30 s). Target gene quantities were normalized to GAPDH/18 S rRNA using the Pfaffl method to determine variations in expression of each target gene under different mineralization conditions. The condition MIM at day 7 was used as calibrator point. Three samples were analysed per group.

2.9. Statistical analysis

Statistical analysis was performed on OriginPro 9.4 (OriginLab, Northampton, MA, USA). Data were compared statistically by one-way analysis of variance (ANOVA) tests. Statistical difference was considered at $p < 0.05$. Data are presented as mean ± standard deviation of mean (SD).

3. Results

The impact of Si-containing medium on hDPSCs was assessed in cell-seeded plastically compressed 3D dense collagen hydrogels, in terms of cell viability and differentiation, mineral deposition and matrix remodelling. Three mineralization conditions were tested: MIM without silicic acid (control), with 10 μM silicic acid (physiological) and 100 μM silicic acid (supraphysiological).

3.1. Influence of silicic acid on hDPSCs viability and metabolic activity

Viability of hDPSCs seeded in collagen hydrogels was assessed using calcein-AM and Ethidium homodimer-1 to stain live and dead cells respectively. Control and silicic acid-treated groups (10 and 100 μM) showed similar high cell viability, with a limited number of dead cells on day 24 of culture (Fig. 1A). Analysis of the virtual volume occupied by cells in the gels showed a significantly greater volume of living cells than dead cells in each group (Fig. 1B). In the presence or absence of Si, live/viable cell volumes were not significantly different.

To evaluate the metabolic activity of the cells, the AlamarBlue® test was carried out over 21 days of culture. The hDPSCs showed a similar trend under the three conditions, with a progressive decrease in resazurin reduction over time (Fig. 1**C**). Cell metabolic activity was not influenced by silicic acid addition over 2 weeks and was slightly higher in Si10-treated cells after 21 days compared to the two other conditions.

3.2. Influence of silicic acid on hDPSCs clustering

The impact of Si on hDPSCs distribution in dense collagen hydrogels was further analysed by SHG and confocal microscopy. On day 24 of differentiation, cells spread out evenly within the collagen matrix cultured in mineralizing medium alone (Fig. 2A). In contrast, Si10-treated matrix exhibited zones of cell clustering, leaving some hydrogel regions without cells (Fig. 2B). This trend was even more marked at Si

Table 1
Primers for real-time PCR.

Primer	Sequence (Forward 5'- 3')	Sequence (Reverse 5'- 3')	Supplier
BGLAP	CAAAGGTGCAGCCTTTGTGTC	TCACAGTCCGGATTGAGCTCA	Roche Diagnostics GmbH, Germany
Col1A1	CCAGTCAGAGTGGCACATCTTGA	GCTCACGATGGTGCCGCTACTA	
MMP13	GCCGGTGTAGGTGTAGATAGGAAA	GGAGATGCCCATTTTGATGATGA	
IBSP	AACGAACAAGGCATAAACGGCACCA	CTTGCCCTGCCTTCCGGTCT	
ALP	GCAGCTTGACCTCCTCGGAAGACACT	TCACCGCCCACCACCTTGTAGCC	
GAPDH	TTGATTTTGGAGGGATCTCG	GAGTCAACGGATTTGGTCGT	
18 S rRNA	TTACAGGGCCTCGAAAGAGT	TGAGAAACGGCTACCACATC	

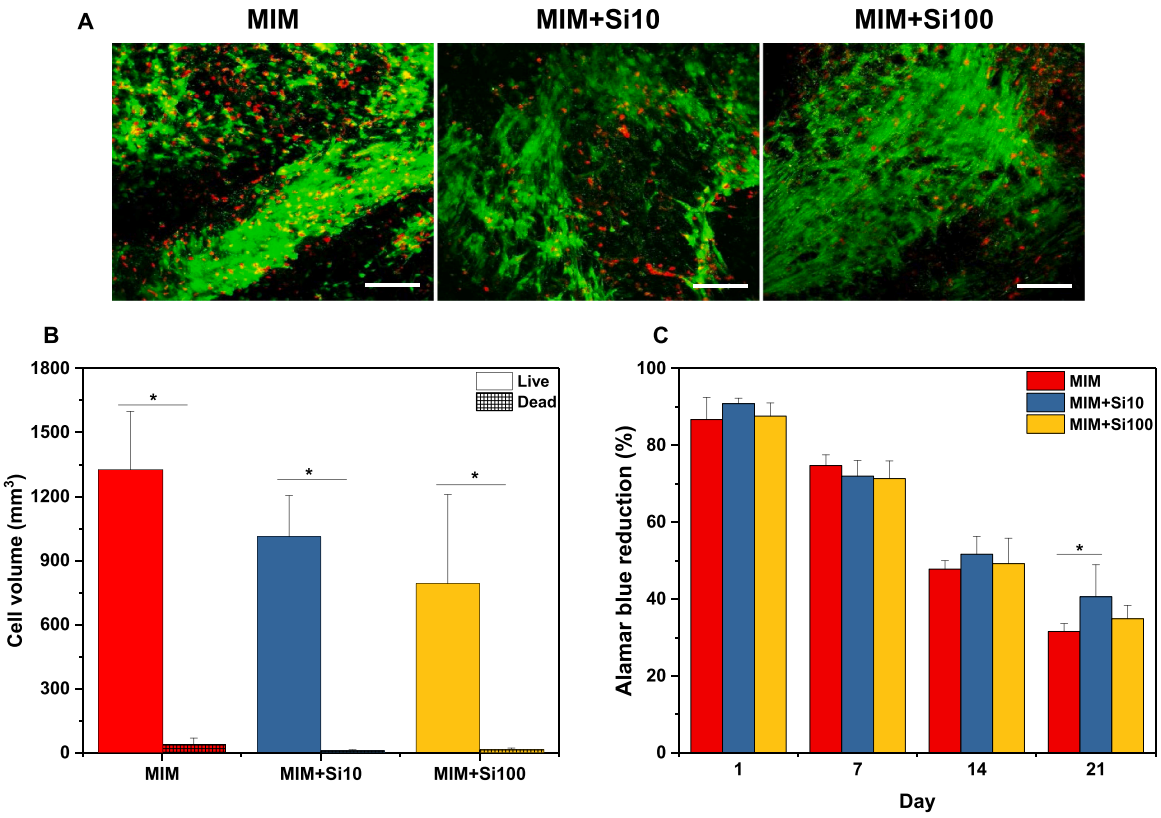

Fig. 1. Viability and metabolic activity of hDPSC seeded in 3D dense collagen gels under mineralizing induction medium (MIM) without or with silicic acid at 10 μM and 100 μM. (A) Confocal images of live/dead stained cells at day 24. Scale bar 100 μm. (B) Quantification of cell volume occupied by live and dead cells in the gels at day 24. (C) Metabolic activity of seeded cells at day 1, 7, 10 and 21 in culture. * $p < 0.05$.

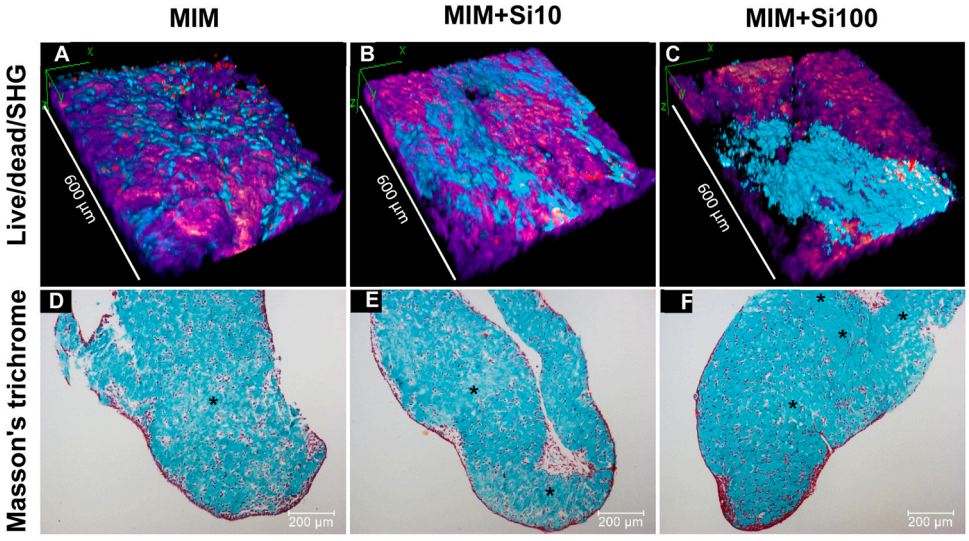

Fig. 2. Cells distribution within the gels on day 24 of growth in absence or presence of Si (10 μM, 100 μM) in Mineralizing Induction Medium (MIM). (A-C) 3D rendering Confocal coupled with SHG images (collagen=purple, live cells=magenta; dead cells=red) and (D-F) Masson's Trichrome staining of scaffolds. Observation of regions without cells (asterisks).

100 μM where a large cell cluster was observed (Fig. 2C). Such cell-free areas could be further visualized on hydrogel cross-sections stained with Masson trichrome (Fig. 2E-F).

3.3. *Influence of silicic acid on hDPSCs proliferation*

hDPSC proliferation in dense collagen hydrogels was assessed by analysing RNA content over a 21 days culture in mineralizing media with or without silicic acid. Cell proliferation increased from day 1 to day 7, then decreased in the three groups independently of the presence of Si (Fig. 3A). A significant difference in RNA content was measured between the Si-100 treated hydrogel and the Si-free group on day 1.

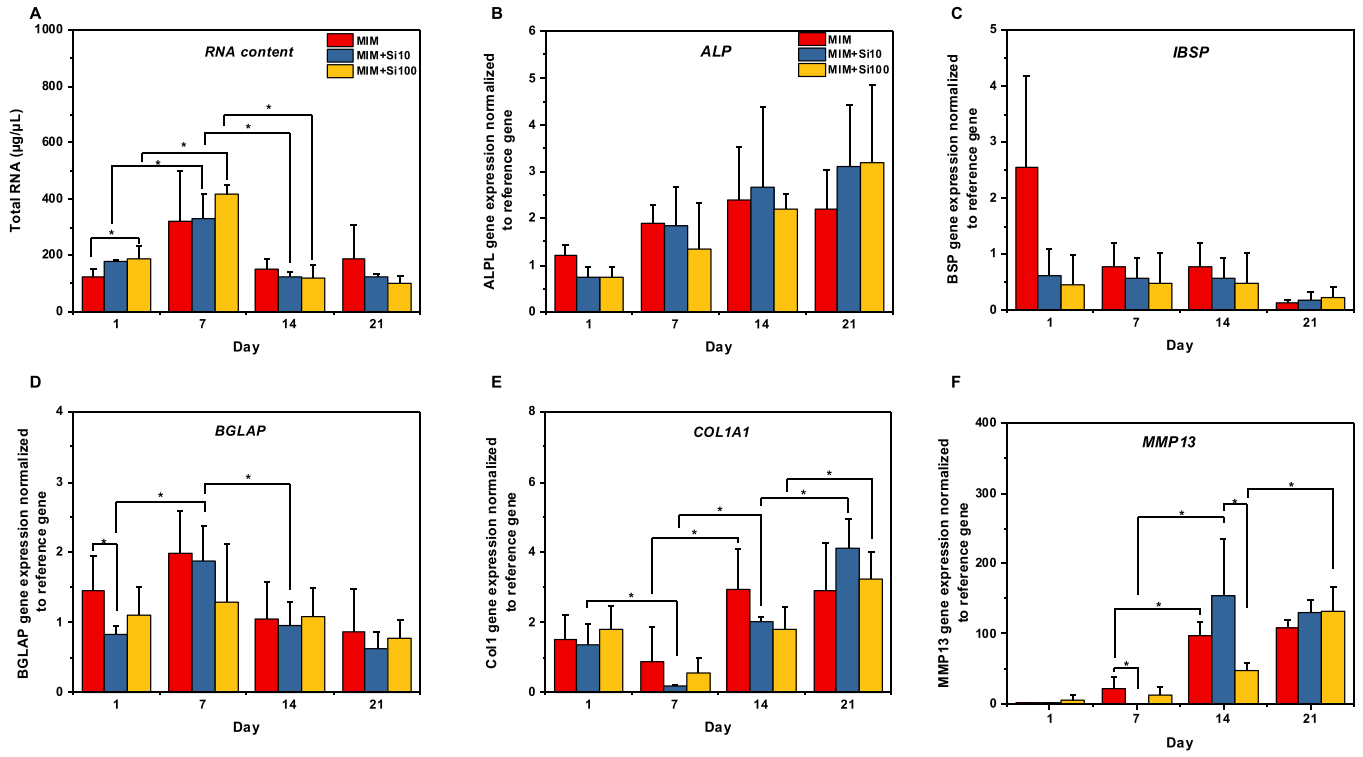

Fig. 3. Influence of Si on hDPSC proliferation, differentiation and matrix remodelling activity after culturing dense cells-laden collagen gels in mineralizing media for 1, 7, 14 and 21 days in the absence or presence of Si (10 µM, 100 µM). (A) RNA content/cell proliferation. Gene expression of *ALP* (B), *BSP* (C), *BGLAP* (D), *COL1A1* (E), *MMP13* (F) by RT-qPCR analysis. * $p < 0.05$.

3.4. Influence of silicic acid on hDPSCs differentiation

Expression of bone- or tooth-related genes, *i.e.* ALP, BSP and BGLAP (osteocalcin), were investigated by RT-qPCR in the hDPSCs cell-laden gels grown for 1, 7, 14 and 21 days in MIM in the absence or presence of Si (10 and 100 µM). All these genes were expressed in both Si- and non-Si-treated groups at all the different time points (Fig. 3B-D).

ALP gene expression (Fig. 3B) followed a similar trend in the control and Si groups, with a progressive increase over time. Comparable low levels of BSP expression were detected in the absence or in the presence or Si from day 1 to day 14, even though on day 1, BSP expression in MIM (without Si) was highly expressed without significant difference *versus* the Si groups (Fig. 3C). BGLAP expression level (Fig. 3D) gradually increased in all the groups from day 1 to day 7, when it reached its highest level, and then decreased dramatically. On day 1, BGLAP was at its lowest level in the Si10 group, and significantly lower compared to the MIM group. Nevertheless, on day 7, BGLAP expression increased up to 2.4-fold in the Si10 group, reaching the same level of expression as in the MIM group. Increasing silicon content (Si100) resulted in a 1.5-fold lower level of BGLAP expression at day 7, albeit no statistically significant difference was observed between the groups.

Complementary immunostaining showed that, at day 24 post-seeding, Nestin, a neural crest mesenchymal stem cells marker [36], was uniformly present throughout the whole width and height of the gels in the three conditions (Fig. 4 A-C). There was a trend of decreasing Nestin-staining intensity with increasing silicon content, but without statistical difference between the three groups (Fig. 4J). In parallel, stronger osteopontin immunolabeling was observed in cell-laden gels grown without Si (Fig. 4D) and with Si10 (Fig. 4E), *vs.* gels grown with Si100 (Fig. 4F). Accordingly, the Si100 group exhibited a significant reduction in the fluorescence intensity of osteopontin (Fig. 4J).

3.5. Mineralization products

3.5.1. Alizarin red S staining

To determine whether the presence of Si in the hydrogels impacted the extent of mineralization, sections of cellularized hydrogels cultured for 24 days were stained with alizarin red. A comparable calcium red staining was observed in MIM alone (Fig. 4G) and Si10 conditions (Fig. 4H), while a fainter and localized staining was observed in Si100 group (Fig. 4I). Noteworthy, the mineral deposits in the Si10-scaffolds were organized in clusters in some areas of the gel (Fig. 4H), in line with the cell organization in clusters already observed in the SHG images (Fig. 2B). In contrast, cross-sectional images of gels grown in MIM alone displayed a uniform distribution of the mineral deposition (Fig. 4G). The presence of phosphate within the same regions was confirmed by Von Kossa staining (Figure SI-1).

3.5.2. SEM imaging and EDS analyses

Cell-mediated matrix mineralization deposition was further analyzed by SEM and EDS, 24 days post-seeding. SEM images clearly indicated that minerals were present along the collagen matrix, and external to the cells, in all the three groups (Fig. 5). In contrast, similarly-treated acellular collagen gels displayed a fibrillar collagen network with no evidence of mineral deposition **(Figure SI-2)**.

EDS analysis of mineralized regions in the 3 culture conditions revealed the presence of both calcium and phosphorus in addition to oxygen and carbon (Fig. 5), while only oxygen and carbon were identified in acellular gels (**SI-2**). The average measured Calcium:Phosphorus ratio was 1.44 ± 0.14 in all samples, confirming the presence of a physiological apatite mineral phase.

3.6. Collagen matrix remodelling

3.6.1. Influence of silicic acid on hDPSCs matrix remodelling activity

Expression matrix remodelling-related genes, *i.e.* MMP13 and Col1,

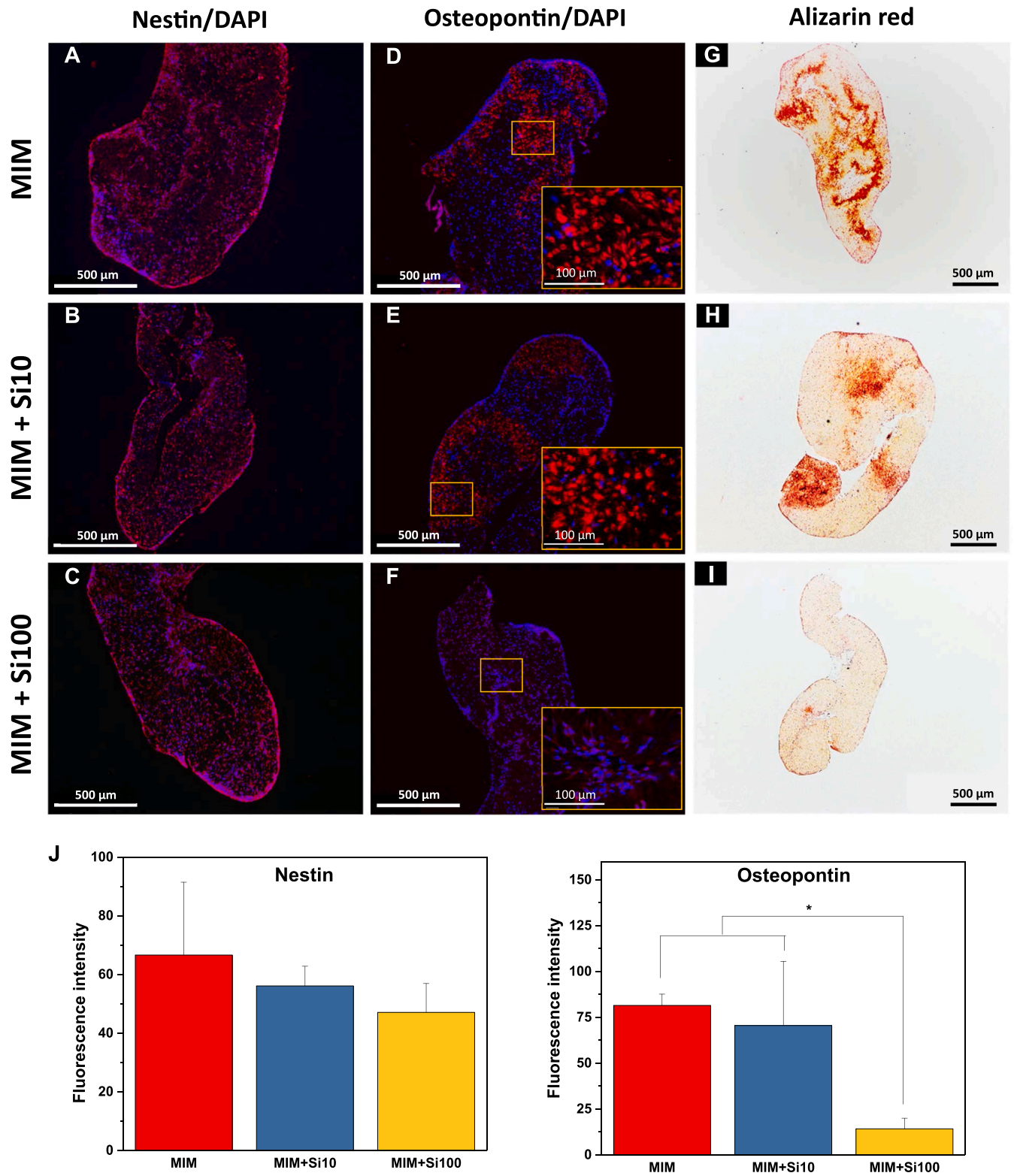

Fig. 4. Histological and immunohistochemical stained sections of hDPSC-seeded scaffolds grown in mineralizing conditions without or with Si (10 µM, 100 µM) for 24 days. (A-C) Nestin/DAPI, (D-F) Osteopontin/DAPI, (G-I) Alizarin red staining and (J) quantifications of Nestin (left) and Osteopontin (right) fluorescence at day 24.

were investigated by RT-qPCR in the hDPSCs cell-laden gels grown for 1, 7, 14 and 21 days in MIM in the absence or presence of Si (10 and 100 µM). Treatment with Si at both concentrations resulted in a time-dependent collagen expression increase from day 7 to day 21, while Col1 levels remained constant between days 14 and 21 in the absence of Si (Fig. 3E). In parallel, MMP 13 expression was low on days 1 and 7 for all groups, with or without Si, and significantly lower for Si10 compared to MIM on day 7 (Fig. 3F). On day 14, Si10 group showed a higher level of MMP13 gene expression compared to the group with Si100, this difference being significant ($p < 0.05$). At day 21, MMP13 gene

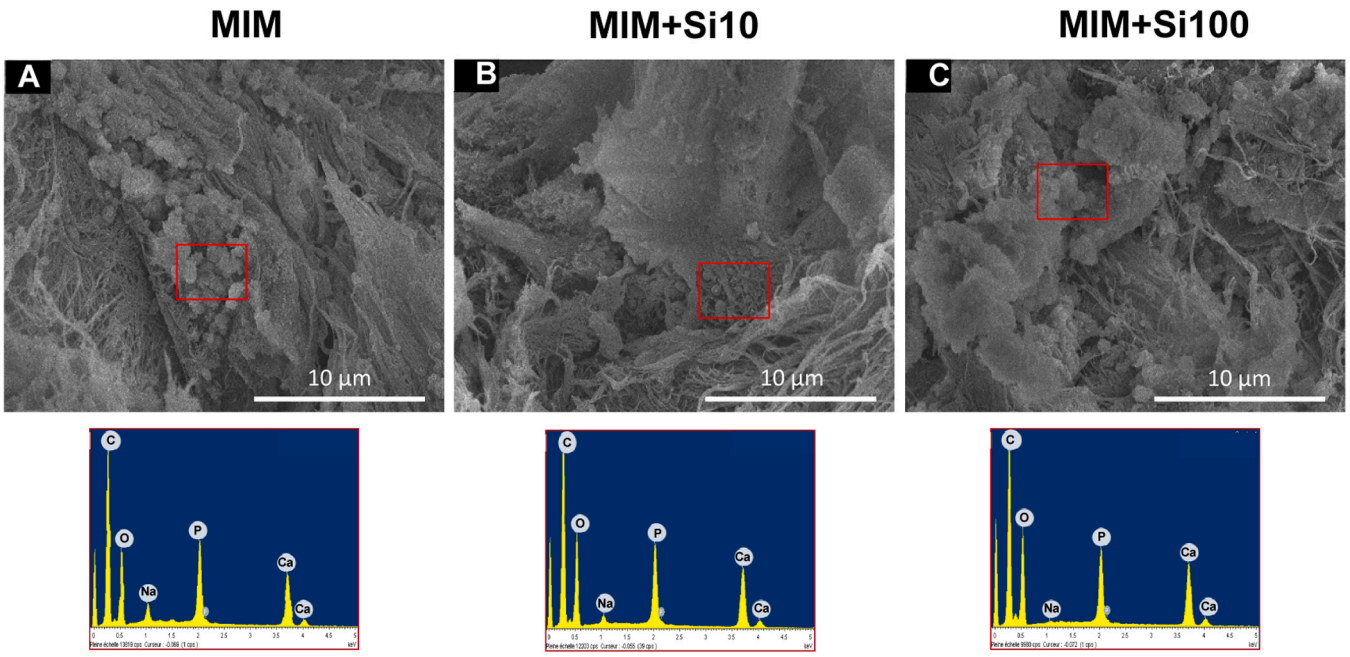

Fig. 5. Mineral formation of dense collagen hydrogels under mineralizing induction medium containing Si (10 µM, 100 µM) or not. (A-C) SEM micrographs and corresponding energy-dispersive x-ray spectra in in the lower panel.

expression continued to increase only for the Si100 condition, reaching values comparable to the other groups.

3.6.2. *Gel contraction*

Relative extents of remodelling activity of collagen hydrogels by hDPSC were assessed by quantifying gel diameter over 14 days of culture and performing SHG microscopy on day 24. hDPSC-seeded gels grown in media without or with Si (10, 100 µM) showed equivalent decreases in diameter/contraction at the same time points (Fig. 6A-B). A reduction in gel diameter of 50 % from its original size was measured on day 1, and then contraction remained relatively constant throughout the 14 days of culture (Fig. 6B). The contractile activity was completely absent in acellular gels, regardless of the presence or absence of Si (Figure SI-3).

3.6.3. *Collagen network structure*

SHG imaging at day 24 of the cell-laden hydrogels grown under the 3 mineralizing conditions (MIM, MIM+Si10, MIM+Si100) highlighted the presence of collagen fibrils, with considerable differences from one

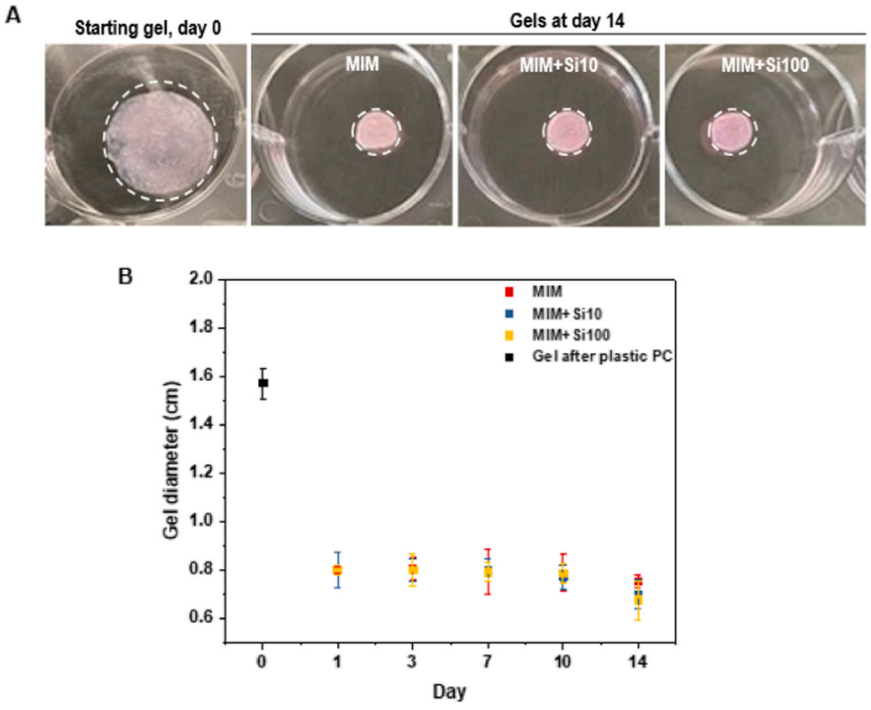

Fig. 6. Contraction of collagen gels by hDPSC in a mineralizing culture medium supplemented with silicon or not. (A) Representative images of type 1 collagen gel contraction at day 14. (B) Average collagen diameter over 14 days of culture.

condition to the others (Fig. 7A).

In MIM alone, individual fibrils were difficult to distinguish and seemed to be assembled in dense ball-like aggregates. In the Si10 condition, some individual fibrils, several tens of micrometers in length, can be visualized. At Si100, such fibrils formed most of the matrix, and seemed to exhibit some local orientation. Noticeably, control gels without cells left for 24 days in MIM displayed much thicker and elongated fibers (**Figure SI-4**).

Quantitative analysis of collagen fibrils orientation and distribution from SHG images confirmed a more pronounced fiber alignment with increasing Si concentration (Fig. 7C). SEM images also suggested a significant variation in fiber alignment recorded at the vicinity of the cells in the different conditions. (Fig. 7B).

4. Discussion

The aim of this work was to identify the possible influence of silicic acid on the behavior of human dental pulp stem cells and, in particular, on their mineralization ability. In fact, whereas similar studies have already been performed using other mineralizing cells in a bone repair context, such as Bone Marrow Stem Cells (BMSCs) and osteoblasts, very little attention has been paid to dental stem cells [22]. In addition, most of these investigations were performed in 2D culture conditions. Here, we hypothesized that providing a tissue-like 3D environment to the cells would offer a more representative model of the *in vivo* situation. Specifically, type I collagen-based dense hydrogels appear particularly promising to produce dentin pulp complexes-like environments [26]. For this study, we selected two silicic acid concentrations, 10 μM (0.28 ppm) which is comparable to the physiological $Si(OH)_4$ concentration [15], and 100 μM (2.8 ppm) to check for possible influence of supraphysiological Si content. Importantly, these concentrations remain well-below the solubility of amorphous silica (*ca.* 2 mM) to prevent the occurrence of silica condensation [31], and are also in the lower concentration range used in comparable studies [22].

Studying the evolution of the metabolic activity of the cells over 3 weeks and evaluating cell viability at the end of the culture time revealed that silicic acid has no toxic effect towards hDPSCs at these concentrations and may even be favorable to cell activity (Fig. 1C). Total RNA content was similar in all conditions and Nestin, a marker of neural crest stem cells which is present both in undifferentiated DPSCs and in the early stages of their osteogenic differentiation [37], was equally present in all samples. This is consistent with previous studies for other cell types showing that, in such a concentration range, Si usually has no effect on cell metabolic activity [22].

Considering gene expression of key mineralization-related proteins, there was no significant difference for *alp* and *bsp* at all concentration and time points. *Bglap* expression was slightly down regulated at day 1 for 10 μM Si but was then similar to all other samples in all conditions. This would suggest that Si has only a minor influence on the odonto/osteogenic differentiation of hDPSCs. In the meantime, SEM/EDS

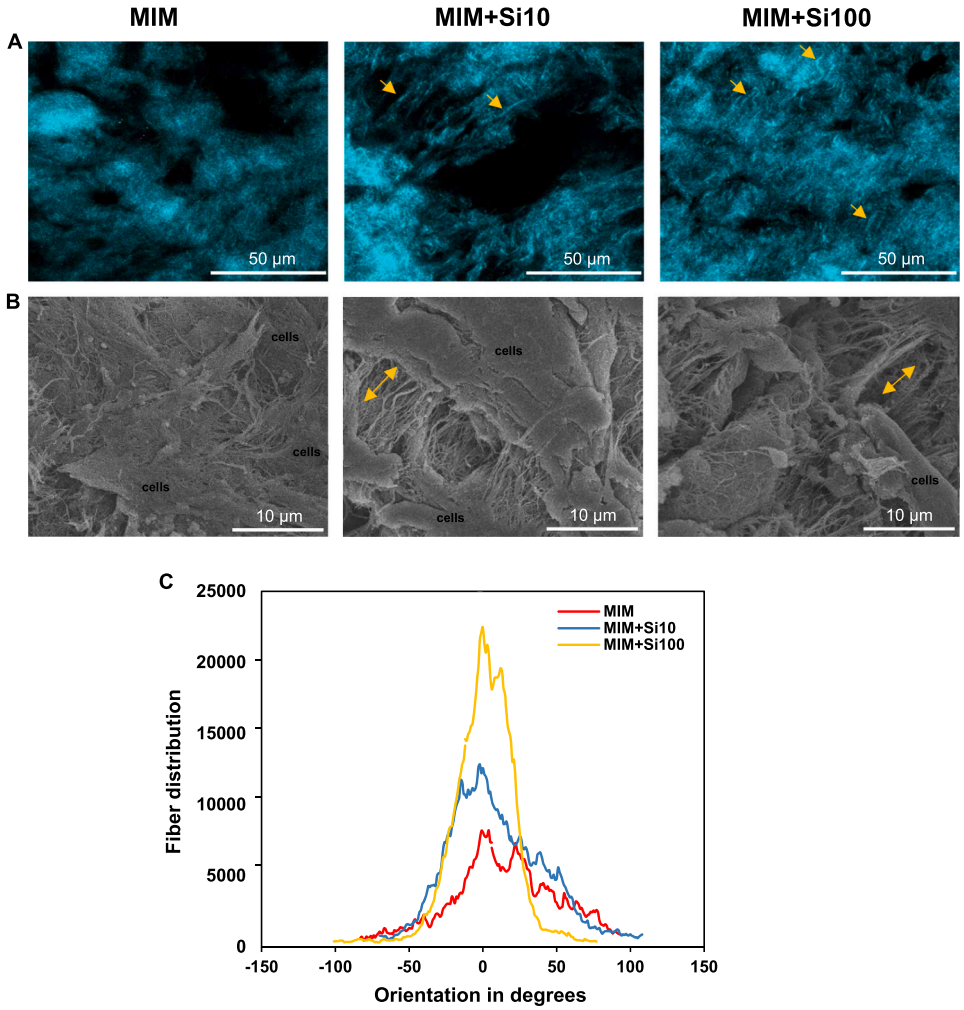

Fig. 7. Matrix structure of hDPSC-seeded dense collagen scaffolds under mineralizing conditions (without and with Si at 10 μM or 100 μM) at 24 days of culture. (A) Second harmonic generation images (individual fibers are highlighted by yellow arrows), (B) SEM micrographs (Fiber alignment is highlighted by yellow arrows) and (C) Quantitative analysis of collagen fiber orientation from SHG.

indicates that the deposited inorganic phase has a Ca/P ratio similar to the expected value for dentin mineral in all conditions, suggesting that Si has no strong effect on the chemistry of hydroxyapatite formation. However, histological analyses revealed a difference in the mineralization extent as shown by an Alizarin red staining much weaker for the 100 μM Si condition compared to the two others. This suggests that despite comparable expression of mineralization-related proteins (ALP, BSP and Osteocalcin), and thus a similar differentiation stage of cells towards an osteogenic phenotype, the mineralization process is somehow inhibited in the presence of a non-physiological, albeit relatively low, Si concentration.

One key difference between the various samples is the state of cell dispersion within the collagen matrix. Indeed, the presence of Si favors the grouping of cells in clusters while, in its absence, hDPSCs are homogeneously distributed within the gels. In parallel, Si appears to favor an organization where the collagen fibrils are more aligned than in its absence. Importantly, the contraction occurring during the first week was equivalent in all the conditions, suggesting that Si has no impact on this initial stage of collagen reorganization. During the course of differentiation, Col1 expression level dropped in all conditions between days 1 and 7, and then increased to reach its largest value in the absence of Si at day 14, while it continued to increase up to day 21 in the presence of Si. Noteworthy, the increase in Col1 expression parallels that of MMP13, one of the main enzymes involved in collagen degradation. Taken together, these data suggest that the presence of silicic acid in the mineralization medium delays matrix remodeling by hDPSCs.

The sequence of 3D matrix remodeling involves the local degradation of the environment, cell migration and deposition of a new matrix [38]. Cell clustering can therefore reflect restricted mobility, due to hindered matrix degradation, poor adhesion and/or limited collagen deposition [39]. This is consistent with the observed delayed MMP13 and Col 1 expression. Moreover, OPN has a key role in cell signaling and migration [40]. Thus, low OPN presence in Si 100 μM conditions may also correlate with limited cell migration. However, understanding the low mineralization yield in this condition is not straightforward. Noticeably, it has been shown that DPSCs from MMP13-knockout mice exhibit reduced mineralization potential [41]. Therefore, low mineralization could correlate with delayed MMP13 expression. Alternatively, it has been recently shown that, although cell aggregation favors mineralization in 2D cultures [42], 3D clustering may orient osteoblast precursor cells differentiation towards osteocyte-like cells with a lower mineralization activity [43].

The next question is to know if this impaired remodeling is due to Si interactions with cells or to a change in the matrix properties leading to unfavorable cell-matrix interactions. Considering the first possibility, it was reported several times that Si promotes the expression of Col1 and mineralizing proteins in osteogenic cells [18], which is in contradiction with our present observations on hDPSCs. However, it has also been previously shown that silica nanoparticles at a 1 mM concentration decreased the expression of proteins involved in cell adhesion (fibronectin, FAK) in normal human dermal fibroblasts, which hinders cell migration and could delay remodeling [44]. The second possibility is that silicic acid establishes some chemical interactions with the collagen molecules and/or fibrils. In this perspective, it was shown that sodium silicate at *ca.* 150 μM could influence type I collagen fibrillogenesis [45]. Here, silicon was not added at the stage of gel formation so that it was not expected to impact the initial scaffold structure. However, interactions of $Si(OH)_4$ with collagen may occur during remodeling where new collagen molecules are synthesized by the cells and undergo fibrillogenesis. The ability of silicic acid solutions to decrease cell adhesion and/or modify the contraction-induced collagen fiber morphology were also reported several times, albeit at higher silicon concentration [31]. At this stage, it is not possible to know which of these mechanisms, which are not exclusive, is responsible for our observations.

Very few similar studies were performed at such low silicon contents, mostly in 2D environments and, to our knowledge, only once with hDPSCs. This study of Miyano and colleagues tested the effects of 5 μM, 50 μM and 500 μM Si supplementation to culture media on hDPSCs [46]. The largest ALP expression was observed on day 14 of culture for all groups, with highest expression at 5 μM Si, but no difference in ALP activity was found between groups. Meanwhile, alizarin red staining was greater with 5 μM and 500 μM Si compared to 50 μM Si on day 28. The latter result is in line with ours, where mineral deposition was more pronounced for the lowest concentration of 10 μM Si than for the supraphysiological Si dose (100 μM). Another study investigating the effects of high Si concentrations on hDPSCs showed that odontoblastic activity, as monitored by ALP activity, DSP expression and alizarin red staining, was improved by 50 ppm Si (2 mM) treatment [47]. However, at this concentration, Si effects can be attributed not only to the bioavailable form of Si (soluble), but also to polymeric forms of Si. In parallel, no difference in hDPSC mineralization was found between cells grown in odontogenic induction medium (OIM) alone and OIM supplemented with 25 ppm Si (1 mM).

Importantly, and contrary to bone, there is, so far, no evidence of a possible physiological role of silicon on dental tissue formation or repair. This can explain why our study reveals little impact of a physiological silicic acid concentration on DPSCs. In contrast, a supraphysiological concentration may result from the dissolution of biomaterials, such as calcium silicates, at the vicinity of the pulp tissue and have a negative impact on reactive dentine formation. Our findings suggest that the released silicic acid would primarily interact with the extracellular matrix rather than with the cells. So far, the contribution of such interactions to the global cell response to silicon at low concentration (*i.e.* below silica solubility) has never been addressed.

In addition, it is important to point out that collagens (mainly type I and type III) constitute only about one third of the pulp matrix composition [48]. Glycosaminoglycans and proteoglycans are present in major amounts and non-collagenous proteins, especially fibronectin, also play a key role in the organization and mechanical properties of the tissue and in cell-matrix interactions. This calls for the development of more physiological pulp-like 3D environments to improve our understanding of DPSCs response to silicon [49]. More globally, such biomimetic platforms could constitute a useful animal-free alternative to current *in vivo* procedures for testing dental biomaterials [50]. However, despite the simplicity of our current model, our study shows that soluble silicon can influence the remineralization potential of dental pulp stem cells, and hence the reparative dentine formation process, through its interactions with the extracellular matrix.

Funding

This work was funded by the French Ministry of Superior Education and Research (Doctorate School 397). This source had no involvement in work conduction and manuscript submission.

Declaration of Competing Interest

The authors declare that they have no known competing financial interests or personal relationships that could have appeared to influence the work reported in this paper.

Acknowledgments

The authors thank J. Dumont (Collège de France, Paris) and Dr F.M. Fernandes (LCMCP) for their assistance in 2PEF/SHG data acquisition and analysis. Help of C. Torrens and B. Baroukh (UR2496) for histological analyses is also acknowledged.

Appendix A. Supporting information

Supplementary data associated with this article can be found in the

online version at doi:10.1016/j.dental.2024.06.021.

References

[1] Manley EB. Pulp reactions to dental cements. Proc R Soc Med 1943;36:488–99.
[2] Zander A. The reaction of dental pulps to silicate cements. J Am Dent Ass 1946;33:1233–43.
[3] Prati C, Gandolfi MG. Calcium silicate bioactive cements: biological perspectives and clinical applications. Dent Mater 2015;31:351–70.
[4] Eskandari F, Razavian A, Hamidi R, Yousefi K, Borzou S. An updated review on properties and indications of calcium silicate-based cements in endodontic therapy. Int J Dent 2022;2022:6858088.
[5] Primus CL, Tay FR, Niu L. Bioactive tri/dicalcium silicate cements for treatment of pulpal and periapical tissues. Acta Biomater 2019;96:35–54.
[6] Song W, Li S, Tang Q, Chen L, Yuan Z. *In vitro* biocompatibility and bioactivity of calcium silicate-based bioceramics in endodontics. Int J Mol Med 2021;48:128.
[7] Kim JM, Choi S, Kwack KH, Kim S-Y, Lee H-W, Park K. G protein-coupled calcium-sensing receptor is a crucial mediator of MTA-induced biological activities. Biomaterials 2017;127:107–16.
[8] Rathinam E, Govindarajan S, Rajasekharan S, Declercq H, Elewaut D, De Coster P, et al. The calcium dynamics of human dental pulp stem cells stimulated with tricalcium silicate-based cements determine their differentiation and mineralization outcome. Sci Rep 2021;11:645.
[9] Kim Y, Lee D, Kim H-M, Kye M, Kim S-Y. Biological characteristics and odontogenic differentiation effects of calcium silicate-based pulp capping materials. Materials 2021;14:4661.
[10] Peng W, Liu W, Zhai W, Jiang L, Li L, Chang J, et al. Effect of tricalcium silicate on the proliferation and odontogenic differentiation of human dental pulp cells. J Endod 2011;37:1240–6.
[11] Cushley S, Duncan HF, Lappin MJ, Chua P, Elamin AD, Clarke M, et al. Efficacy of direct pulp capping for management of cariously exposed pulps in permanent teeth: a systematic review and meta-analysis. Int Endod J 2021;54:556–71.
[12] Wu B-C, Kao C-T, Huang T-H, Hung CJr, Shie M-Y, Chung H-Y. Effect of verapamil, a calcium channel blocker, on the odontogenic activity of human dental pulp cells cultured with silicate-based materials. J Endod 2014;40:1105–11.
[13] Wu T, Xu C, Du R, Wen Y, Chang J, Huan Z, et al. Effects of silicate-based composite material on the proliferation and mineralization behaviors of human dental pulp cells: An *in vitro* assessment. Dent Mater J 2018;37:889–96.
[14] Peng W, Huan Z, Pei G, Li J, Cao Y, Jiang L, et al. Silicate bioceramics elicit proliferation and odontogenic differentiation of human dental pulp cells. Dent Mater J 2022;41:27–36.
[15] Jugdaohsingh R. Silicon and bone health. J Nutr Health Aging 2007;11:99–110.
[16] Henstock JR, Canham LT, Anderson SI. Silicon: the evolution of its use in biomaterials. Acta Biomater 2015;11:17–26.
[17] Götz W, Tobiasch E, Witzleben S, Schulze M. Effects of silicon compounds on biomineralization, osteogenesis, and hard tissue formation. Pharmaceutics 2019;11:117.
[18] Reffitt DM, Ogston N, Jugdaohsingh R, Cheung HFJ, Evans BAJ, Thompson RPH, et al. Orthosilicic acid stimulates collagen type 1 synthesis and osteoblastic differentiation in human osteoblast-like cells in vitro. Bone 2003;32:127–35.
[19] Shie M-Y, Ding S-J, Chang H-C. The role of silicon in osteoblast-like cell proliferation and apoptosis. Acta Biomater 2011;7:2604–14.
[20] Kim EJ, Bu SY, Sung MK, Choi MK. Effects of silicon on osteoblast activity and bone mineralization of MC3T3-E1 Cells. Biol Trace Elem Res 2013;152:105–12.
[21] Zhou X, Moussa FM, Mankoci S, Ustriyana P, Zhang N, Abdelmagid S, et al. Orthosilicic acid, $Si(OH)_4$, stimulates osteoblast differentiation in vitro by upregulating miR-146a to antagonize NF-κB activation. Acta Biomater 2016;39:192–202.
[22] Turner J, Nandakumar A, Anilbhai N, Boccaccini AR, Jones JR, Jell G. The effect of Si species released from bioactive glasses on cell behaviour: a quantitative review. Acta Biomater 2023;170:39–52.
[23] Han P, Wu C, Xiao Y. The effect of silicate ions on proliferation, osteogenic differentiation and cell signalling pathways (WNT and SHH) of bone marrow stromal cells. Biomater Sci 2013;1:379–92.
[24] Duval K, Grover H, Han LH, Mou Y, Pegoraro AF, Fredberg J, et al. Modeling physiological events in 2D vs. 3D cell culture. Physiology 2017;32:266–77.
[25] Griffanti G, Nazhat SN. Dense fibrillar collagen-based hydrogels as functional osteoid-mimicking scaffolds. Int Mater Rev 2020;64:502–21.
[26] Coyac BR, Hoas B, Chafey P, Falgayrac G, Slimani L, Rowe PS, et al. Defective mineralization in X-Linked hypophosphatemia dental pulp cell cultures. J Dent Res 2018;97:184–91.
[27] Troka I, Griffanti G, Canaff L, Hendy GN, Goltzman GN, Nazhat SN. Effect of menin deletion in early osteoblast lineage on the mineralization of an in vitro 3D osteoid-like dense collagen gel matrix. Biomimetics 2022;7:101.
[28] Coyac BR, Chicatun F, Hoac B, Nelea V, Chaussain C, Nazhat SN, et al. Mineralization of dense collagen hydrogel scaffolds by human pulp cells. J Dent Res 2013;92:648–54.
[29] Chamieh F, Collignon AM, Coyac BR, Lesieur J, Ribes S, Sadoine J, et al. Accelerated craniofacial bone regeneration through dense collagen gel scaffolds seeded with dental pulp stem cells. Sci Rep 2016;6:38814.
[30] Mbitta Akoa D, Sicard L, Hélary C, Torrens C, Baroukh B, Poliard A, et al. Role of physico-chemical and cellular conditions on the bone repair potential of plastically-compressed collagen hydrogels. Gels 2024;10:130.
[31] Heinemann S, Coradin T, Desimone MF. Bio-inspired silica-collagen materials: applications and perspectives in the medical field. Biomater Sci 2013;1:688–702.
[32] Gronthos S, Mankani M, Brahim J, Robey PG, Shi S. Postnatal human dental pulp stem cells (DPSCs) in vitro and in vivo. Proc Natl Acad Sci USA 2000;97:13625–30.
[33] Gobeaux F, Mosser G, Anglo A, Panine P, Davidson P, Giraud-Guille MM, et al. Fibrillogenesis in dense collagen solutions: a physicochemical study. J Mol Biol 2008;376:1509–22. 376.
[34] Brown R, Wiseman M, Chuo CB, Cheema U, Nazhat SN. Ultrarapid engineering of biomimetic materials and tissues: fabrication of nano- and microstructures by plastic compression. Adv Funct Mater 2005;15:1762–70.
[35] Bancelin S, Decencière E, Machairas V, Albert C, Coradin T, Schanne-Klein M-C, et al. Fibrillogenesis from nanosurfaces: multiphoton imaging and stereological analysis of collagen 3D self-assembly dynamics. Soft Matter 2014;10:6651–7.
[36] Lendahl U, Zimmerman LB, McKay RD. CNS stem cells express a new class of intermediate filament protein. Cell 1990;60:585–95.
[37] Di Benedetto A, Posa F, Carbone C, Cantore S, Brunetti G, Centonze M, et al. NURRI downregulation favors osteoblastic differentiation of MSCs. Stem Cells Int 2017;2017:7617048.
[38] Harjanto D, Zaman MH. MH modeling extracellular matrix reorganization in 3D environments. PLoS ONE 2013;8:e52509.
[39] Schultz KM, Kyburz KA, Anseth KS. Measuring dynamic cell-material interactions and remodeling during 3D human mesenchymal stem cell migration in hydrogels. Proc Natl Acad Sci USA 2015;112:E3757–64.
[40] Sodek J, Ganss B, McKee MD. Osteopontin. Crit Rev Oral Biol Med 2000;11:279–303.
[41] Duncan HF, Kobayashi Y, Yamauchi Y, Quispe-Salcedo A, Chao Feng Z, Huang J, et al. The critical role of MMP13 in regulating tooth development and reactionary dentinogenesis repair through the wnt signaling pathway. Front Cell Dev Biol 2022;10:883266.
[42] A.J. Deegan, H.M. Aydin, B. Hu, S. Konduru, J.H. Kuiper, Y. Yang. A facile in vitro model to study rapid mineralization in bone tissues. BioMed Eng OnLine 13 (2014) 136.
[43] Kim J, Adachi T. Cell condensation triggers the differentiation of osteoblast precursor cells to osteocyte-like cells. Front Bioeng Biotechnol 2019;7:288.
[44] Zhang Y, Hu L, Yu D, Gao C. Influence of silica particle internalization on adhesion and migration of human dermal fibroblasts. Biomaterials 2010;31:8465–74.
[45] Eglin D, Shafran KL, Livage J, Coradin T, Perry CC. Comparative study of the influence of several silica precursors on collagen self-assembly and of collagen on 'Si' speciation and condensation. J Mater Chem 2006;16:4220–30.
[46] Miyano Y, Mikami M, Katsuragi H, Shinkai K. Effects of Sr^{2+}, BO_3^{3-}, and SiO_3^{2-} on Differentiation of human dental pulp stem cells into odontoblast-like cells. Biol Trace Elem Res 2023;201:5585–600.
[47] Alsenan J, Chou L. Effect of silicon and calcium on human dental pulp cell cultures. Int J Mater Sci Appl 2017;6:290–6.
[48] Linde A. The extracellular matrix of the dental pulp and dentin. J Dent Res 1985;64:523–9.
[49] Hadjichristou C, Papachristou E, Bonovolias I, Bakopoulou A. Three-dimensional tissue engineering-based Dentin/Pulp tissue analogue as advanced biocompatibility evaluation tool of dental restorative materials. Dent Mater 2020;36:229–48.
[50] Tran XV, Gorin C, Willig C, Baroukh B, Pellat B, Decup F, et al. Effect of a calcium-silicate-based restorative cement on pulp repair. J Dent Res 2012;91:1166–71.